Chapter 3

Frequency stability in the resilience context

3.1 Introduction

The energy system transition for achieving the target of limiting the global warming to 1.5 °C requires a massive increase of electricity generation from renewable energysources [23]. Many studies conducted in recent years predict an exponential increase of wind and solar PV generation in the coming decades. The installed capacity of inverter based wind and solar PV generation is expected to be at least tenfold in 2050 compared to current installed renewable generation capacity [23]–[25]. This massive increase in inverter based generation will lead to the deterioration of system inertia in the long term jeopardizing the stability of the future network due to the predicted phasing out of fossil fuel based power generation [26].

Large-scale transmission grid investments are required for the connection of remote renewable generation sources to the existing grid on the one hand, and to increase the transmission capacity of the existing system for allowing the transport of renewable energy to demand centers on the other. HVDC is a widely used technology for transmission grid expansion, and the future transmission grid is expected to evolve towards a hybrid AC/DC grid. According to the European Network of Transmission System Operators (ENTSO-e), 59 % of the planned transmission system investments in the coming decade will utilize HVDC technology [27]. Classical line commutated (LCC) HVDC technology has widely been used for bulk transmission over large distances and for submarine transmission. In the last decade voltage source converter (VSC) based HVDC has commonly been utilized for connecting offshore wind farms, but also for onshore power transmission due its various advantages such as reactive power support, power flow control capability and the improvement of the system stability by means of

oscillation damping and grid forming control [28]–[30]. Especially, fast frequency reserve provision, e.g., in form of virtual inertia, using voltage source converters can help to improve the stability of the grid in low inertia systems [30], [31].

Considering the hybrid nature of the future grid and the expected impact of inverter based generation on the system stability, planning and operational scheduling models for generation and transmission assets need to consider system stability constraints as well as various control possibilities of these assets for system stability improvement. The value that HVDC systems can bring with respect to fast frequency reserve provision by positively affecting the allowable loss of infeed in the grid is a sparsely researched field. Tosatto et. al demonstrate the value of sharing frequency containment reserves (FCR) utilising emergency power control functionality of HVDC links [32]. Huang et. al. perform an analysis based on historical data on HVDC available interconnector capacity to compare different methods for providing fast frequency reserve, in particular the application of droop control for HVDC converters and the exchange of frequency containment reserves [33]. Kaushal et. al. use a simplified market model and a fixed dimensioning incident, e.g., maximum loss of infeed to demonstrate the value of inertia support from HVDC [34]. In the aforementioned studies, the dimensioning incident to determine the volume of required reserves has been based on a fixed value, and potential outages of HVDC systems themselves have not been taken into account.

To conduct a detailed analysis of the operational benefits of utilising HVDC systems, and grids, the operational scheduling of the generation assets and their capabilities with respect to ramping and frequency control need to be modeled. This is typically done by utilizing economic dispatch and unit commitment models [35]. For quantifying the impact of frequency stability, security constrained unit commitment (SCUC) models have been developed [36], although SCUC can also refer to the consideration of network contingencies. Wu et. al. use a Monte Carlo based approach and include linearised network security constraints in the unit commitment problem [37], whereas Fu et. al. also consider spinning reserve and AC network constraints [38], however, with a fixed amount of the spinning reserves. Ahmadi and Ghasemi use linearised system frequency limit constraints in the unit commitment model resulting in a mixed integer linear problem [39]. Chang et. al. utilize fast frequency response and frequency regulating reserve requirements in the unit commitment model [40], and Wen et. al. investigate the effects of battery storage systems by adding rate of change frequency and frequency nadir constraints in the unit commitment problem which is formulated as a mixed integer problem [41]. However, both models neglect network constraints. Similarly Markovic et. al. use a linear lower

bound on the minimum system frequency for analysing the effect of fast frequency response of storage in low inertia grids [42]. Many of the works on security constrained unit commitment (SCUC) models thus focus only on a purely AC system and only consider generator outages or an increase in demand as a source of frequency events. However, such an approach is not sufficient for future hybrid AC/DC grids.

Only few works have approached the unit commitment problem with explicit representation of hybrid AC/DC networks. Isuru et. al. use a convex relaxation of the AC/DC network equations to embed them in the unit commitment problem and solve it for a large scale AC/DC network [43]. Bahrami et. al. use an algorithmic approach to solve the SCUC problem for a modified version of the IEEE 30 bus system with renewable energy sources connected with point-to-point and multi-terminal HVDC links [44]. Further, Zhang et al. use minimum frequency and voltage stability constraints and utilize Benders cuts to subsequently solve the unit commitment problem and the operational subproblems to enforce the stability constraints [45]. However, the analysis in [45] is only limited to a small network and point-to-point HVDC links connecting remote generation.

Another important aspect is that tie line contingencies leading to system splits often impact the system in a more severe way as shown by Püschel-Løvengreen et. al. where maximum frequency deviation and rate of change of frequency constraints have been considered [46]. However, this approach has only been applied to AC tie lines, and to systems asynchronously connected via HVDC links, such as in the North Sea region.

Summarizing, most available literature thus presents the following gaps: (1) The economic benefits of providing fast frequency reserves with HVDC are not well quantified, and only analyzed for fixed dimensioning incidents (2) security constrained unit commitment models are not applied to large AC/DC networks, and especially not HVDC grids, (3) tie line outages are often not considered in the problem despite their potential for causing very large power and frequency deviations.

The remainder of this section outlines an optimisation model for quantifying benefits brought by fast frequency reserve provision through HVDC systems for extending existing cost benefit analysis methodologies, where the system stability impact is often considered in a qualitative way. The optimisation model minimises the total operational costs of the system by optimally scheduling HVDC links in AC/DC grids and ensuring sufficient headroom for fast frequency reserve provision. This minimizes the inertia requirement for the grid by implicitly determining the largest loss of infeed, and allows a higher share of renewable generation in the grid. The main features of the described model and implementation are:

1. A stability and security constrained unit commitment model for hy-

brid AC/DC networks, considering generator, storage, AC and DC grid contingencies.

2. Implicit determination of the dimensioning incident, i.e., maximum loss of infeed, the inertia need and reserve volume in a dynamic way considering available renewable generation and load demand.

3. Two comprehensive case studies to demonstrate real life applicability of the developed model.

4. An open-source implementation of the developed model as a software package in Julia language.

3.2 Frequency control principles

Frequency control services are defined based on the time frame within which the services are provided as depicted in fig. 3.1. Inertia support is the instantaneous response of the power system components such as synchronous generators and loads to frequency deviations. In the case of synchronous machines, this is attributed to the release or absorption of kinetic energy in cases of system disturbances attributed to the loss of infeed or load increase, as the mechanical inertia of synchronous machines counteracts the variation of their rotational speed caused by the acceleration or deceleration of the machines due to the energy imbalance in the system. A power system with high system inertia limits the rate of change of frequency (RoCoF).

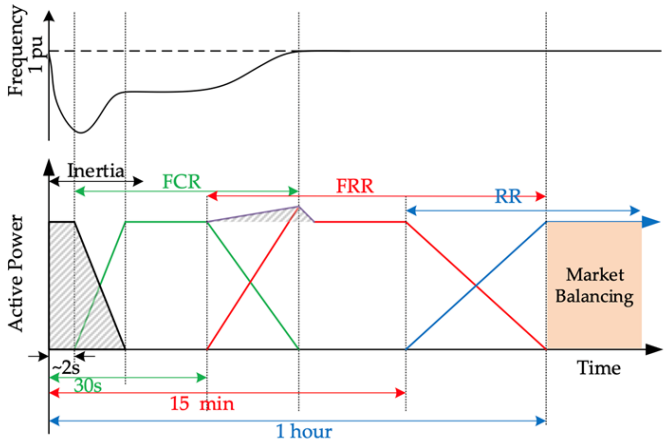

Figure 3.1: Frequency control ancillary services activation time [47]

The reduction of the system inertia due to increase in inverter-based generation is seen as a threat to the operation of power networks which can be

counteracted by utilising fast frequency reserves (FFR). Frequency containment reserves (FCR) or often referred to as primary reserves are activated for disturbances lasting for a few seconds. FCR is provided according to a defined power/frequency droop of generators, or energy storage systems and is usually activated for a very limited time (several minutes) while the active power set points of the generators remain unchanged.

Frequency restoration reserves (FRR) or secondary reserves are activated to bring the frequency back to its nominal value. This is done by actively changing the set points of generators (or demand) within a given control zone, such that the interzonal exchanges are restored to pre-contingency values. Replacement reserves or tertiary reserves are active power reserves supporting FRR in anticipation of further possible system imbalances that can last over an extended time period (several hours or days). Such reserves are usually activated manually and are optimized by the TSO.

Benefits of HVDC and MVDC: High and medium voltage DC systems (links and grids) can be utilized to provide frequency control ancillary services over a variety of time frames. Voltage source converters can perform a full power flow reversal within a few hundred milliseconds [48], such that they can be used to provide fast frequency reserves. Furthermore, high voltage source converters are in general foreseen with a power / frequency droop characteristic acting in the same way as generating units. To provide frequency restoration reserves (FRR and RR), the active power set points of HVDC converters can be adjusted by system operators.

Requirements: The aim of utilizing frequency control services is to counteract energy imbalance in a synchronously connected system. This can be achieved in fundamental ways. Firstly, energy from outside the synchronous zone can be provided, for which HVDC links connecting asynchronous networks can be utilized. However, in such set-ups, the provision of energy for the synchronous zone with energy deficit will also result in an imbalance in the zone that provides the energy, which needs to be compensated by the inertial response and FCR provision by the generators of the system providing the service. This type of service then requires cross-border coordination.

The second way to counteract energy imbalance is to release stored energy from within the synchronous area, which can be achieved with DC systems with embedded storage [49]. Frequency support provided through DC links or grids must be coordinated with the DC voltage control to limit interactions, since both functionalities depend on active power. Coordinated frequency support schemes within a DC grid can be implemented considering communications between the AC/DC converters [50] or without communications and relying on local measurements [51]. AC/DC converters can implement frequency support schemes considering both grid-following or grid-forming controls, but the dynamic responses and AC/DC interactions

will be different.

3.3 Modeling frequency control and stability

3.3.1 Frequency stability constraints

In this section, we summarize some typical frequency stability constraints for considered in [52] as follows:

- Reserve requirements

  This constraint is defined as

  $$\sum_{g \in \mathcal{G}} r_g^{t,\rho} \geq R_{t,\rho}^{min}, \quad \forall t \in \mathcal{T} \tag{3.1}$$

  where ρ is FCR, FRR, or RR. This constraint ensures that the system has adequate reserves of any kind at all time.

- Dynamic allocation reserve

  $$\sum_{g \in \mathcal{G} \setminus \{g_k\}} r_g^{t,FCR} - p_{g_k,t} \geq 0, \quad \forall g_k \in \mathcal{G}, t \in \mathcal{T} \tag{3.2}$$

  Compared to (3.1), in this constraint, the N-1 criterion is defined dynamically in the optimization. The sum of the reserve in every N-1 set of units must be greater than the production level of each single unit. This means that each set of generator units must be able to compensate for the loss of one of the units.

- Fixed inertia and kinetic energy requirement

  $$\sum_{g \in \mathcal{G}} H_g u_g \geq H_{min}, \quad \forall t \in \mathcal{T} \tag{3.3}$$

  A constraint can be placed on the sum of the inertia constant (H_i) of on-line units as expressed in (3.3) or, on their kinetic energy (KE) at nominal frequency, where S_g is the nominal apparent power of unit g.

- RoCoF constraint

  $$\sum_{g \in \mathcal{G} \setminus \{g_k\}} S_g H_g u_{g,t} \geq \frac{f^{nom} p_{g_k,t}}{2 f_{slope}^{max}}, \quad \forall g_k \in \mathcal{G}, t \in \mathcal{T} \tag{3.4}$$

  The maximal rate of change of frequency (f_{slope}^{max}) occurs in the first instant of the disturbance and it depends only on the size of the disturbances and the kinetic energy storage in the on-line units.

3.3.2 Frequency-constrained unit commitment

3.3.2.1 Mathematical model formulation

The stability constrained unit commitment problem is formulated as a two stage problem, where the first stage represents the unit commitment and dispatch decisions for thermal generators, (pumped) hydro storage generators, and the set point schedules for the HVDC connections under normal operating conditions, i.e., the N-0 case. The second stage approximates the frequency deviation based on the rate of change of frequency (RoCoF) for the largest possible contingency and applies a minimum allowable system frequency constraint to limit it. The first stage is subject to the power flow equations and limits typically associated with optimal power flow models, which have been formulated using the well known 'DC power flow' approximation. Both stages are linked by the generator commitment decisions for the determination of the available grid inertia and the generator dispatch and AC and DC tie line flows for the determination of the largest loss of infeed. As such, the generator dispatch and the AC and DC tie line flows are limited based on their impact on the frequency deviation. Further, the fast frequency response contribution from HVDC converters connecting different synchronous areas (both in N-0 and N-1 contingency cases) is modelled using a set of linear constraints. Similarly, the frequency containment reserve provision through generators and HVDC converters is linearly approximated as well. The resulting model is a mixed-integer linear programming model which can efficiently be solved by state-of-the-art solvers.

The objective of the optimisation is to minimize the total operational costs of the system consisting of power generation costs and potential demand curtailment costs under the normal operating conditions. Furthermore, costs for fast frequency reserve provision by HVDC converters and frequency containment reserves by thermal generators and (pumped-hydro) storage generators during contingency conditions are considered in order to avoid reserve provision for non binding contingencies, as the transfer energy from the non contingent zone to the contingent zone would also result in a frequency deviation in the non contingent zone. The objective function is thus formulated as

$$\begin{aligned} min \sum_{t\in T}(\sum_{g\in G}\beta_{g,t}C_g^{start-up} + P_{g,t}C_g + \alpha_{g,t}C_g^0 + \sum_{s\in S}P_{s,t}^{dch}C_s^{dch} + \sum_{l\in L}P_{l,t}^{curt}VOLL_l + \\ \sum_{c\in C}(\sum_{d\in D}|\Delta P_{d,c,t}^{ac}|C_d^{ffr} + \sum_{g\in G}|\Delta P_{g,c,t}|C_g^{fcr} + \sum_{s\in S}|\Delta P_{s,c,t}|C_s^{fcr})), \end{aligned} \tag{3.5}$$

where $\beta_{g,t}$ is the start-up decision for generator g at time t, $P_{g,t}$ is its dispatch value, and $\alpha_{g,t}$ is its on-off status to account the no-load operating costs C_g^0.

$P^{dch}_{s,t}$ represents the amount of power injection from (pumped) hydro storage into the grid with the associated cost C^{dch}_{s}. $VOLL_l$ represents the value of lost load for potential demand curtailment $P^{curt}_{l,t}$. $|\Delta P^{ac}_{d,c,t}|$ represents the change in the power dispatch value for the HVDC converter d for providing fast frequency response during contingency c. C^{ffr}_{d} is a cost to avoid unnecessary HVDC converter actions for non binding contingencies, which could realistically be chosen as the anticipated market price for fast frequency response provision [53]. Similarly, $\Delta P_{g,c,t}$ and $\Delta P_{s,c,t}$ denote the change in the output thermal and (pumped) hydro generators, respectively, for providing frequency containment reserves, with their associated costs C^{fcr}_{g} and C^{fcr}_{s}. The cost for frequency containment reserve provision can be obtained from data sources such as [54]

First stage model for normal operating conditions In the first stage the model is constrained by the well known 'DC' optimal power flow equations for the AC and DC grids

$$\theta_{ref,t} = 0 \; \forall t \in T \tag{3.6}$$

$$\sum_{g \in G_i} P_{g,t} + \sum_{d \in D_i} P^{ac}_{d,t} - \sum_{l \in L_i} P_{l,t} + \sum_{s \in S_i} P_{s,t} = \sum_{(i,j) \in \mathcal{E}_i} P^{ac}_{ij,t} \; \forall i \in \mathcal{I}^{ac}, t \in T \tag{3.7}$$

$$P^{ac}_{ij,t} = B_{ij}(\theta_{i,t} - \theta_{j,t}) \; \forall (i,j) \in \mathcal{E}^{ac}, t \in T \tag{3.8}$$

$$\underline{P^{ac}_{ij}} \leq P^{ac}_{ij,t} \leq \overline{P^{ac}_{ij}} \; \forall (i,j) \in \mathcal{E}^{ac}, t \in T \tag{3.9}$$

$$\underline{\theta_{ij}} \leq (\theta_i - \theta_j) \leq \overline{\theta_{ij}} \; \forall (i,j) \in \mathcal{E}^{ac}, t \in T \tag{3.10}$$

$$\alpha_{g,t}\underline{P_{g,t}} \leq P_{g,t} \leq \alpha_{g,t}\overline{P_{g,t}} \; \forall g \in G, t \in T \tag{3.11}$$

$$\underline{P_{l,t}} \leq P_{l,t} \leq \overline{P_{l,t}} \; \forall l \in L, t \in T \tag{3.12}$$

$$P^{curt}_{l,t} + P_{l,t} = P^{ref}_{l,t} \; \forall l \in L, t \in T \tag{3.13}$$

$$\sum_{d \in D_i} P^{dc}_{d,t} = \sum_{(i,j) \in \mathcal{I}^{dc}_i} P^{dc}_{ij,t} \forall i \in \mathcal{I}^{dc}, t \in T \tag{3.14}$$

$$\underline{P^{ac}_{d}} \leq P^{ac}_{d,t} \leq \overline{P^{ac}_{d}} \; \forall d \in D, t \in T \tag{3.15}$$

$$\underline{P^{dc}_{d}} \leq P^{dc}_{d,t} \leq \overline{P^{dc}_{d}} \; \forall d \in D, t \in T \tag{3.16}$$

$$P^{dc}_{d,t} + P^{ac}_{d,t} = 0 \; \forall d \in D, t \in T \tag{3.17}$$

$$\underline{P^{dc}_{ij}} \leq P^{dc}_{ij,t} \leq \overline{P^{dc}_{ij}} \; \forall (i,j) \in \mathcal{E}^{dc}, t \in T, \tag{3.18}$$

where (3.6) enforces an angle of zero degree for the reference buses, (3.7) represents the AC node active power balance, (3.8) represents the power flow through AC lines connecting nodes i and j using the line admittance B_{ij} and the nodal voltage angles θ_i and θ_j. The line flows are bounded by (3.9),

and (3.10) provides limits for the nodal voltage angle differences. (3.11) and (3.12) provide limits for the generation and demand, which can be different for each considered time point considering variable generation and demand. Demand shedding is modelled using (3.13), where $P_{l,t}^{ref}$ is the reference demand at time t for load l. The DC grid power balance at each DC node is enforced by (3.14) where $P_{d,t}^{dc}$ is the DC side power of HVDC converter d and $P_{ij,t}^{dc}$ are the power flows on the DC lines connected to DC node i. (3.15) and (3.16) define limits for the AC and DC side power injections of HVDC converters and (3.17) assumes lossless converters. Finally (3.18) sets limits for the power flows on DC branches which are modelled using a network flow model when linearised [15].

The unit commitment constraints for generators are modelled using the well-known one binary formulation as outlined in [55],

$$P_{g,t} - P_{g,t-1} \leq \Delta P_{g,t}^{up} + (\underline{P_{g,t}} - \Delta P_{g,t}^{up})\beta_{g,t} \; \forall g \in G, t \in T \tag{3.19}$$

$$P_{g,t-1} - P_{g,t} \leq \Delta P_{g,t}^{down} + \underline{P_{g,t}}\gamma_{g,t} \; \forall g \in G, t \in T \tag{3.20}$$

$$1 - \alpha_{g,t} \geq \sum_{\tau=t+1-MDT_g} \gamma_{g,\tau} \; \forall g \in G, t \in T \tag{3.21}$$

$$\alpha_{g,t} \geq \sum_{\tau=t+1-MUT_g} \beta_{g,\tau} \; \forall g \in G, t \in T \tag{3.22}$$

$$\alpha_{g,t-1} - \alpha_{g,t} + \beta_{g,t} - \gamma_{g,t} = 0 \; \forall g \in G, t \in T \tag{3.23}$$

$$\alpha_{g,t} \in \{0,1\}, \beta_{g,t}, \gamma_{g,t} \in [0,1] \; \forall g \in G, t \in T, \tag{3.24}$$

where (3.19) and (3.20) represent the upwards and downwards ramping constraints for the generators, (3.21) and (3.22) model the minimum down and up times, respectively, and (3.23) and (3.24) model the start-up ($\beta_{g,t}$) and shut-down ($\gamma_{g,t}$) decisions.

As for the commitment of (pumped) hydro storage generators we use a more simplified model with on-off constraints.

$$\underline{P_s^{ch}}\alpha_{s,t} \leq P_{s,t}^{ch} \leq \overline{P_s^{ch}}\alpha_{s,t} \;\; \forall s \in S, t \in T \tag{3.25}$$

$$\underline{P_s^{dch}}\alpha_{s,t} \leq P_{s,t}^{dch} \leq \overline{P_s^{dch}}\alpha_{s,t} \;\; \forall s \in S, t \in T, \tag{3.26}$$

where $\alpha_{s,t}$ denotes the commitment status of (pumped) hydro storage generators, $P_{s,t}^{ch}$ denotes the charging power for the storage asset, whereas $P_{s,t}^{dch}$ denotes the discharging power. According to the convention chosen in (3.7), the power seen at point of common coupling is $P_{s,t} = P_{s,t}^{dch} - P_{s,t}^{ch}$. We enforce the state-of-charge continuity with,

$$E_{s,t} = E_{s,t-1} + \Delta t(P^{ch}\eta_{s,t}^{ch} - \frac{P_{s,t}^{dch}}{\eta_s^{dch}}) \; \forall s \in S, t \in T, \tag{3.27}$$

where η_s^{ch} and η_s^{dch} represent the charging and discharging efficiency. In order to keep the problem formulation linear, we are not using binary decision variables for charging / discharging exclusivity, as due to cost of storage discharge in the objective function, and selecting $\eta_s^{ch} < 1$ and $\eta_s^{dch} < 1$, the simultaneous charging and discharging is inherently penalised. Δt denotes the time interval of the simulation, for which throughout this work, one hour has been chosen. Furthermore, the energy content of the storage $E_{s,t}$ is subject to limits,

$$\underline{E_{s,t}} \leq E_{s,t} \leq \overline{E_{s,t}} \quad \forall s \in S, t \in T. \tag{3.28}$$

Second stage model for N-1 contingency conditions Each possible generator, storage or HVDC converter[1] contingency causes a power and frequency deviation in the synchronous zone it is connected to [26]. For tie line contingencies, a frequency deviation will occur on both sides of the tie line [46]. A frequency drop is observed in the zone where power was imported into, and a frequency increase is observed in the zone where power was exported from. The reaction of the system due to a deficiency in the power balance is depicted in Figure 3.2-top [56]. All generators connected in the grid will respond to the frequency event based on their inertia, limiting the drop of the frequency. Usually, also the power consumption of the loads decreases with the frequency providing additional damping [57], which is not modeled in this case study. The frequency keeps decreasing until the point where frequency containment reserves (FCR), i.e, the primary generator responses are fully deployed at which point the minimum system frequency is reached, and the frequency is restored up to a steady-state frequency deviation further mitigated by secondary and tertiary reserves. In Figure 3.2, f_{min} is the lower bound of the minimum frequency if the system inertia is constant during the inertial response. In this work we are modelling the response from HVDC converters, generator and storage assets both in the time interval between the outage occurring and the start of FCR provision by generators $[T_0, T'_{FCR}] = \Delta T^{ffr}$, as well as the time interval to fully deploy FCR, $[T'_{FCR}, T''_{FCR}] = \Delta T^{fcr}$, respectively.

The initial rate of change of frequency (RoCoF) in each modelled zone z can be calculated using [57]

$$\frac{df_{z,t}}{dt} = \frac{\Delta P_{z,c,t}}{2 \cdot E_{z,t}^{tot}} \quad \forall z \in Z, t \in T, \tag{3.29}$$

where $\Delta P_{z,c,t}$ is the power deviation observed in zone z, caused by contingency c and $E_{z,t}^{tot}$ is the total system inertia of zone z which is determined by the conventional and (pumped) hydro generators which are online, and

[1] In cases of connections to a different synchronous zone

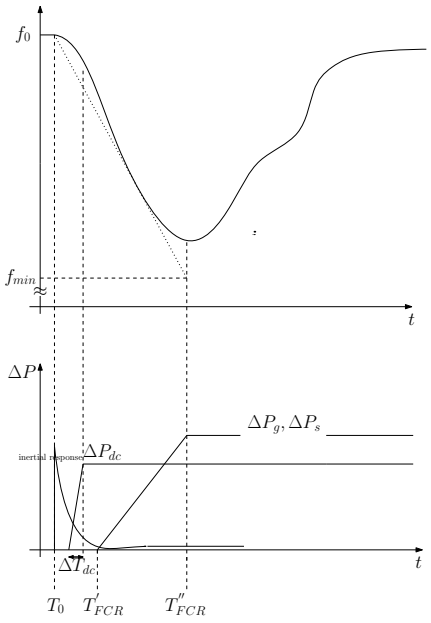

Figure 3.2: Frequency deviation due to a generator, storage, tie line or HVDC converter contingency, and the inertial response, FFR and FCR contributions of HVDC converters, generators and storage devices

thus also not contingent, for a given time point t, e.g.,

$$E^{tot}_{z,t} = \sum_{g_z \in G} \alpha_{g_z,t} H_{g_z,t} + \alpha_{s_z,t} H_{s_z,t} \quad \forall s_z \in S_z \backslash \{c\}. \tag{3.30}$$

We use the RoCoF, which is typically limited between 0.1 and 1 Hz/s to linearly approximate the maximum frequency deviation in the transient phase before the full deployment of FCR, thus $\Delta T = \Delta T^{ffr} + \Delta T^{fcr}$, which is an overestimation as proposed in [42]. As such, we can write the frequency deviation constraint for each possible contingency $c \in C$ as follows:

$$\underline{\Delta f} \leq f_0 \frac{\Delta P_{z,c,t} \Delta T}{2 \cdot E^{tot}_{z,t}} \leq \overline{\Delta f} \quad \forall z \in Z, c \in C, t \in T, \tag{3.31}$$

where f_0 is the nominal grid frequency, and $\underline{\Delta f}$ and $\overline{\Delta f}$ are minimum and maximum frequency limits, respectively.

The fast frequency reserve response of HVDC links is modelled according to Figure 3.2-bottom where it is assumed that the HVDC link can linearly increase power injection into the grid with a power deficit. We assume that the converters provide fast frequency reserve after a minimum frequency deviation, e.g., a dead band of f_{db}. Solving for the area under the curve pro-

vides the total energy contribution of the DC link which can be written as:

$$E^{dc}_{ffr} = \Delta P^{dc} \cdot min(1, \frac{\Delta T^{ffr}}{\Delta T^{dc}}) \cdot \frac{min(\Delta T^{ffr}, \Delta T^{dc})}{2} + \Delta P^{dc} \cdot max(0, \Delta T^{ffr} - \Delta T^{dc}) \; \forall d \in D \backslash \{c\}, \tag{3.32}$$

where the ΔP^{dc} is the fast set point change of the DC converter, and ΔT^{dc} is the ramp rate for fast frequency reserve provision, e.g., the time until the HVDC converter fully reach its rated power, which is typically in the order of a few hundred milliseconds [58]. Note that for all HVDC converter contingencies $E^{dc}_{ffr} = 0$ and formulation used in (3.32) also allows to define values $\Delta T^{dc} \geq \Delta T^{ffr}$ for slower ramp rates.

Thus, accounting the for fast frequency reserve contribution from HVDC, we can modify (3.31) as follows:

$$\underline{\Delta f} + f_{db} \leq f_0 \frac{\Delta P_{z,c,t} \Delta T^{ffr} - E^{dc}_{ffr}}{2 \cdot E^{tot}_{z,t}} \leq \overline{\Delta f} - f_{db} \; \forall z \in Z, c \in C, t \in T, \tag{3.33}$$

In the time interval between the start of the FCR deployment, and in its full utilisation, ΔT^{fcr}, the frequency reserve contributions of HVDC converters, E^{dc}_{fcr}, conventional generators, E^{g}_{fcr} and (pumped) hydro generators, E^{s}_{fcr} can be calculated as follows:

$$E^{dc}_{fcr} = \Delta P^{dc}_{d,c,t} \Delta T^{fcr} \; \forall d \in D \backslash \{c\} \tag{3.34}$$

$$E^{g}_{fcr} = \frac{\Delta T^{fcr} \Delta P_{g,c,t}}{2} \; \forall g \in G \backslash \{c\} \tag{3.35}$$

$$E^{s}_{fcr} = \frac{\Delta T^{fcr} \Delta P_{s,c,t}}{2} \; \forall s \in S \backslash \{c\} \tag{3.36}$$

Note that for contingent converters, conventional and pumped hydro storage generators, $E^{dc,s,g}_{fcr} = 0$. Furthermore, conventional and (pumped) hydro generators are bound by their ramping rates,

$$P_{g,t} - r_g \Delta T^{fcr} \leq \Delta P_{g,c,t} \leq P_{g,t} + r_g \Delta T^{fcr} \; g \in G, t \in T \tag{3.37}$$

$$P_{s,t} - r_s \Delta T^{fcr} \leq \Delta P_{s,c,t} \leq P_{s,t} + r_s \Delta T^{fcr} \; s \in S, t \in T, \tag{3.38}$$

where r_g and r_s are the ramp rates of conventional and (pumped) hydro generators in MW/s, respectively.

Eventually, by also enforcing

$$\underline{\Delta f} + f_{db} \leq f_0 \left(\frac{\Delta P_{z,c,t} (\Delta T^{ffr} + \Delta T^{fcr})}{2 \cdot E^{tot}_{z,t}} - \frac{E^{dc}_{ffr} + E^{dc}_{fcr} + E^{g}_{fcr} + E^{s}_{fcr}}{2 \cdot E^{tot}_{z,t}} \right) \leq \overline{\Delta f} - f_{db} \; \forall z \in Z, c \in C, t \in T, \tag{3.39}$$

we can ensure that the minimum grid frequency constraint holds over the entire time frame until the full deployment of the frequency containment reserves. Note that the correct sign of the power injections and absorptions need to be used for the different AC tie line and HVDC contingencies, as well as for the HVDC contribution to correctly model the frequency increase/decrease for each affected zone.

Contingency constraints In the optimisation model we define four different variables representing the power deviation per synchronous zone and time point caused by an outage of the different asset types, namely a thermal generator contingency, $\Delta P^{cg}_{z,t}$, a (pumped hydro) storage contingency, $\Delta P^{cs}_{z,t}$, a tie line contingency[2], $\Delta P^{cl}_{z,t}$ and an HVDC converter contingency $\Delta P^{cd}_{z,t}$. We introduce following constraints to make sure that the power deviation during contingencies represents the largest possible contingency

$$P_{g_z,t} \leq \Delta P^{cg}_{z,t} \quad \forall g_z \in G_z, t \in T \tag{3.40}$$
$$|P_{s_z,t}| \leq \Delta P^{cs}_{z,t} \quad \forall s_z \in S_z, t \in T \tag{3.41}$$
$$|P_{l_z,t}| \leq \Delta P^{cl}_{z,t} \quad \forall l_z \in L_z, t \in T \tag{3.42}$$
$$|P_{d_z,t}| \leq \Delta P^{cd}_{z,t} \quad \forall d_z \in D_z, t \in T, \tag{3.43}$$

where the sets $X_z, X \in \{G, S, L, D\}$ denote the set of assets belonging to a given synchronous zone z. Note that constraints (3.33) and (3.39) need to be enforced for all asset types, zones and time points, where $\Delta P_{z,c,t}$ in those expression are replaced with the above defined power deviations $\Delta P^{c}_{x,z,t}$ with $x \in \{g, s, l, d\}$.

As indicated in equations (3.30) and (3.32) - (3.36), the total inertia of the system is determined by the commitment status of thermal and (pumped) hydro storage generators, and furthermore only assets that are not selected as the largest contingency in the system can provide FFR and FCR services. To that end, we define binary indicator variables for generator, (pumped) hydro generator, tie line and HVDC converters to identify which of the assets would result in being the largest contingency, e.g., the largest loss of infeed in zone z. We impose the following constraints,

[2]This contingency is only defined if a tie line would cause a system split

$$\sum_{g_z \in G_z} \delta_{g_z,t} = 1 \;\; \forall z \in Z, t \in T \tag{3.44}$$

$$\sum_{s_z \in S_z} \delta_{s_z,t} = 1 \;\; \forall z \in Z, t \in T \tag{3.45}$$

$$\sum_{l_z \in L_z} \delta_{l_z,t} = 1 \;\; \forall z \in Z, t \in T \tag{3.46}$$

$$\sum_{d_z \in D_z} \delta_{d_z,t} = 1 \;\; \forall z \in Z, t \in T \tag{3.47}$$

$$(\delta_{g_z,t} - 1)M \leq \Delta P^{cg}_{z,t} - P_{g_z,t} \leq (1 - \delta_{g_z,t})M \;\; \forall z \in Z, t \in T \tag{3.48}$$

$$(\delta_{s_z,t} - 1)M \leq \Delta P^{cs}_{z,t} - P_{s_z,t} \leq (1 - \delta_{s_z,t})M \;\; \forall z \in Z, t \in T \tag{3.49}$$

$$(\delta_{l_z,t} - 1)M \leq \Delta P^{cl}_{z,t} - P_{l_z,t} \leq (1 - \delta_{l_z,t})M \;\; \forall z \in Z, t \in T \tag{3.50}$$

$$(\delta_{d_z,t} - 1)M \leq \Delta P^{cd}_{z,t} - P_{d_z,t} \leq (1 - \delta_{d_z,t})M \;\; \forall z \in Z, t \in T, \tag{3.51}$$

where (3.44) - (3.51) make sure that only one contingency is selected, whereas (3.48) - (3.51) make sure that the power deviation of the selected contingency equals to power dispatch value of the asset selected as the contingency. M is a large enough value such that the dispatch values of the non-selected assets are not restricted. Using the contingency indicator variables we update (3.30) by

$$E^{tot}_{z,t} = \sum_{g_z \in G} (\alpha_{g_z,t} - \delta_{g_z,t}) H_{g_z,t} + (\alpha_{s_z,t} - \delta_{s_z,t}) H_{s_z,t} \quad \forall s_z \in S_z \backslash \{c\}, \tag{3.52}$$

and also by bounding the FFR and FCR contributions of all generator and converter assets

$$(1 - \delta_{g_z,t})\underline{\Delta P_{g,c,t}} \leq \Delta P_{g,c,t} \leq (1 - \delta_{g_z,t})\overline{\Delta P_{g,c,t}} \tag{3.53}$$

$$(1 - \delta_{s_z,t})\underline{\Delta P_{s,c,t}} \leq \Delta P_{s,c,t} \leq (1 - \delta_{s_z,t})\overline{\Delta P_{s,c,t}} \tag{3.54}$$

$$(1 - \delta_{d_z,t})\underline{\Delta P^{dc}_{d,c,t}} \leq \Delta P^{dc}_{d,c,t} \leq (1 - \delta_{d_z,t})\overline{\Delta P^{dc}_{d,c,t}}, \tag{3.55}$$

we make sure that contingent assets can not provide any contribution.

By linking the generator and HVDC converter power set point changes to the set points under the normal operating condition, and enforcing appropriate limits we can ensure that enough headroom is reserved for frequency reserve provision,

$$\underline{P_g} \leq P_{g,t} + \Delta P_{g,c,t} \leq \overline{P_g} \; \forall g \in G, c \in C, t \in T \tag{3.56}$$

$$\underline{P_s} \leq P_{s,t} + \Delta P_{s,c,t} \leq \overline{P_s} \; \forall s \in S, c \in C, t \in T \tag{3.57}$$

$$\underline{P^{dc}_d} \leq P^{dc}_{d,t} + \Delta P^{dc}_{d,c,t} \leq \overline{P^{dc}_d} \; \forall d \in D, c \in C, t \in T. \tag{3.58}$$

Furthermore, by enforcing the DC grid power flow equations in the second stage, we can enforce that the injection of energy into one zone inherently results in energy absorption from the other zone, as the energy balance needs to be preserved:

$$\sum_{d \in D_i} P^{dc}_{d,c,t} = \sum_{(i,j) \in \mathcal{I}^{dc}_i} P^{dc}_{ij,c,t} \quad \forall i \in \mathcal{I}^{dc}, c \in C, t \in T. \tag{3.59}$$

This way, the fast frequency reserve provision between multiple zones connected by a meshed HVDC grid can be modeled as well.

Summarizing, the final optimisation model consists of the objective (3.5), the first stage unit commitment, dispatch and power flow constraints (3.6) - (3.28), frequency limit constraints (3.33), (3.39), (3.52), reserve contribution constraints (3.32), (3.34) - (3.36), contingency constraints (3.40) - (3.51), limits of FFR and FCR contribution (3.37), (3.38), (3.53) - (3.58) and HVDC grid energy balance constraint (3.59).

3.3.3 Uncertainty handling in frequency-constrained unit commitment using adaptive robust optimization

3.3.3.1 Two-stage robust unit commitment

This case study is based on a two-stage robust optimization framework since we are interested in protecting the system against the worst-case generator outage with respect to the total operational cost. This cannot be done using a stochastic programming approach since it needs to take into account the probability of a generator outage and calculates the total expected cost. Such an approach would yield less robust outcomes and it is simultaneously difficult to obtain accurate probability values for generator outages.

In general, robust optimization methods have been presented in numerous studies and applications. For power system applications, this approach has been implemented for the unit commitment problem [59]–[62] using continuous uncertainty sets such as demand and wind generation. In [62] the contingency of generators and transmission lines is incorporated into the uncertainty sets in addition to the wind uncertainty. In [63], the outages of lines and renewable generation are modeled as stochastic variables. Another application of robust UC with discrete uncertainties is presented in [64] by allowing mixed-integer recourse using quick-start units.

The similarity of the uncertainty realization in the previously mentioned papers comes from the outage realization in the operational problem. In this case study, the contingency is applied as a security layer, in the form of rate-of-change-of-frequency (RoCoF), without necessarily realizing the contingency in the operational problem [52]. This means that the contingency